# MATERIALS PROCESSING FUNDAMENTALS 2023

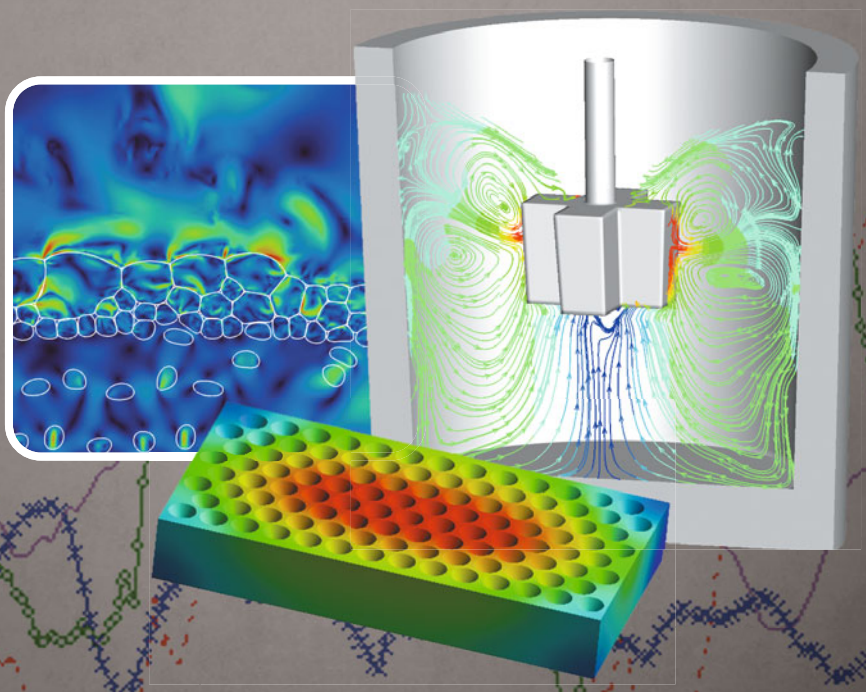


EDITED BY
Samuel Wagstaff
Alexandra Anderson
Adrian S. Sabau



TMS

Springer

# The Minerals, Metals & Materials Series

Samuel Wagstaff · Alexandra Anderson ·
Adrian S. Sabau
Editors

# Materials Processing Fundamentals 2023

TMS

Springer

*Editors*
Samuel Wagstaff
Oculatus Consulting
Marietta, GA, USA

Alexandra Anderson
Gopher Resource
Tampa, FL, USA

Adrian S. Sabau
Oak Ridge National Laboratory
Oak Ridge, TN, USA

ISSN 2367-1181 ISSN 2367-1696 (electronic)
The Minerals, Metals & Materials Series
ISBN 978-3-031-22656-4 ISBN 978-3-031-22657-1 (eBook)
https://doi.org/10.1007/978-3-031-22657-1



Cover Illustration: Left: From Chapter "Toward Meso-scale Modelling of Slag Foaming Phenomena in Pyrometallurgy", Quinn G. Reynolds et al., Figure 5: Dispersed-phase marker phases and velocities for ug = 0.02 m/s case. https://doi.org/10.1007/978-3-031-22657-1_10. Right: From Chapter "Effect of Wearing Impellers on Multiphase Flow and Desulfurization During KR Mechanical Stirring Process", Wei Chen et al., Figure 3: Effect of the number of employed heats of the impeller on the distribution of flow pattern, a initial state, b after employed 120 heats, c after employed 220 heats. https://doi.org/10.1007/978-3-031-22657-1_2. Bottom: From Chapter "Simulation of Ferroalloy Casting in Copper Moulds", Haifei An et al., Figure 8: Temperature field of the mould at 50 s before demoulding. https://doi.org/10.1007/978-3-031-22657-1_18.

This Springer imprint is published by the registered company Springer Nature Switzerland AG
The registered company address is: Gewerbestrasse 11, 6330 Cham, Switzerland

# Preface

The symposium Materials Processing Fundamentals is hosted at the Annual Meeting of The Minerals, Metals & Materials Society (TMS) as the flagship symposium of the Process Technology and Modeling Committee. It is a unique opportunity for interdisciplinary presentations and discussions about, among others, processing, sensing, modeling, multi-physics, computational fluid dynamics, and thermodynamics.

The materials covered include ferrous and non-ferrous elements, and the processes range from mining unit operations to jointing and surface finishing of materials. Acknowledging that modern processes involve multi-physics, the symposium and its proceedings allow the reader to learn the methods and outcome of other fields' modeling practices, often enabling the development of practical solutions to common problems. Modeling of basic thermodynamic and physical properties plays a key role, along with computational fluid dynamics and multi-phase transport and interface modeling.

Contributions to the proceedings include applications such as steel processing, modeling of steel and non-ferrous alloys treatments for properties control, multi-physics, and computational fluid dynamics modeling for molten metal processes and properties measurement. Extractive, recovery, and recycling process modeling is also presented, completing a broad view of the field and practices of modeling in materials processing.

The engagement of TMS and committee members to chair sessions and review manuscripts makes this symposium and its proceedings possible. The editor and co-editors acknowledge the invaluable support and contribution of these volunteers as well as TMS staff members, in particular, Patricia Warren, Trudi Dunlap, and Matt Baker.

Samuel Wagstaff
Alexandra Anderson
Adrian S. Sabau

# Contents

**Part VI Poster Session**

# About the Editors

**Samuel Wagstaff** is currently a partner at Oculatus Consulting, specializing in aluminum processing and product development. He holds degrees in Mechanical Engineering from Cornell University (B.S.) and Materials Science from MIT (M.S., Sc.D.). Previously as the Lead Scientist at Novelis, he led new product and process development for the entire R&D ecosystem across three continents. Currently, Dr. Wagstaff focuses on increasing profitability and productivities of non-ferrous products by process improvement and fundamental research. He has helped to design over 1 million tons of recycle capacity in the aluminum sector and is the author of over 35 patents. Sam is currently serving as the principal investigator on a $1M ReMADE grant to develop technology to improve the recyclability of organic laden aluminum scrap.

**Alexandra Anderson** Ph.D., PMP, is an R&D manager at Gopher Resource, LLC, an environmental solutions company specializing in lead battery recycling. Her work focuses on driving furnace productivity and efficiency initiatives through computational fluid dynamic (CFD) modeling and implementing novel equipment designs. Currently, she is also the principal investigator for a DOE HPC4Manufacturing partnership between Gopher Resource and Oak Ridge National Lab investigating high-fidelity multi-phase furnace modeling. Alexandra obtained her B.S. in Mechanical Engineering from Gonzaga University and her M.S. and Ph.D. in Metallurgical and Materials Engineering from the

Colorado School of Mines. Her dissertation investigated fluid flow and thermal profiles within secondary lead reverberatory furnaces using CFD techniques. Alexandra is active in The Minerals, Metals & Materials Society (TMS), where she serves as the vice-chair of the Process Technology and Modeling Committee; she was also the recipient of the 2021 TMS Extraction and Processing Division (EPD) Young Leader Award. Her scholarly activities include nine peer-reviewed publications, co-editorships of seven special topics for JOM, as well as several podium presentations at national conferences.

**Adrian S. Sabau** received an Engineer Diploma in Mechanical and Materials Processing from the University of Craiova, Romania, and a Ph.D. degree in Mechanical Engineering from Southern Methodist University in 1996. In 1999, Dr. Sabau joined Oak Ridge National Laboratory as a Research Staff Member of Materials Science and Technology, where he worked as a Senior Research Staff Member from 2008. Since 2018, Dr. Sabau has been a Computational Materials Scientist in the Computational Sciences & Engineering Division. Dr. Sabau seeks to advance the materials processing, metal casting, photonic processing, and materials for energy applications through the development of computational fluid dynamics and experimental methodologies for the property measurement, process analysis, and materials behavior in response to conditions experienced in service. Dr. Sabau is an ASME fellow, and ASM fellow, and the recipient of three R&D 100 awards in process sciences. He was granted 7 patents and has published 169 technical papers.

# Part I
# Process Optimization

# Modeling of Macro-scale Reaction Effects in a Secondary Lead Reverberatory Furnace


**Nicholas J. Walla, Emily A. Higley, Armin K. Silaen, Alexandra Anderson, Joseph Grogan, and Chenn Q. Zhou**

**Abstract** A long-standing and effective way to recycle lead-acid battery materials is through processing of lead compounds into lead product within a reverberatory furnace. Exploration of process and design changes through unit modification can be costly, time-consuming, and potentially harmful to operational efficiency. Modeling of process behavior, including furnace heat transfer and material reduction/decomposition, can however be difficult. To this end, a method for reflecting the production capabilities of a lead reverberatory furnace under various operational conditions has been developed. Reactions of the lead compounds have been approximated within a steady-state computational fluid dynamics simulation by adding or removing heat from the domain depending on local thermal conditions. With this, process and design changes can be explored in the simulated environment before moving onto more-advanced stages of modeling or experimentation.

**Keywords** Reverberatory furnace · Lead recycling · Numerical modeling · Pyrometallurgy

N. J. Walla (✉) · E. A. Higley · A. K. Silaen · C. Q. Zhou
Center for Innovation through Visualization and Simulation, Purdue University Northwest, 2200 169th Street, Hammond, IN 46323, USA
e-mail: njwalla@pnw.edu

E. A. Higley
e-mail: ehigley@pnw.edu

A. K. Silaen
e-mail: asilaen@pnw.edu

C. Q. Zhou
e-mail: czhou@pnw.edu

A. Anderson · J. Grogan
Research and Development, Gopher Resource, 6505 Jewel Avenue, Tampa 33619, FL, USA
e-mail: Allie.Anderson@GopherResource.com

J. Grogan
e-mail: Joe.Grogan@GopherResource.com



S. Wagstaff et al. (eds.), *Materials Processing Fundamentals 2023*, The Minerals, Metals & Materials Series, https://doi.org/10.1007/978-3-031-22657-1_1

## Introduction

Nearly 80% of lead produced within the United States comes from the recycling of scrap lead [1], with nearly half of global lead production being secondary lead produced from lead-acid battery recycling [2]. The dominant method for producing secondary lead is via pyrometallurgical processes in reverberatory furnaces, with 78% of secondary lead produced in the United States using reverberatory furnaces [3]. The growth of secondary lead production brings with it efforts to optimize the process and minimize any environmental impacts. For overall lead production (both primary and secondary), the smelting of secondary lead is a strong contributor to the global warming impact of the lead industry [4], hence the importance of optimization and energy reduction.

Research into reverberatory furnaces has been ongoing for decades using a variety of approaches. Experimental furnaces have been built to examine the specifics of operational behavior, such as the modular furnace design of King et al. [5]. Their modular furnace, in this case an aluminum reverberatory furnace, allowed for exploration of the material heat absorption based on surface area, the effects of combustion space volume changes, the impact of wall emissivity on overall heat flux, and various furnace input and output relationships. Kumar et al. [6] built an experimental furnace to explore the effect of flame impingement on the solid charged material, working to identify the effective heat transfer through the charge material under different furnace conditions. This effort was combined with a computational fluid dynamics (CFD) simulation of the furnace to further explore design and operation conditions.

Numerical modeling of pyrometallurgical furnaces is an attractive alternative to experimentation. Constructing and operating experimental furnaces can be prohibitively expensive or outright impossible in some instances. Experimentation on production furnaces risks damage, lost time, and negative impacts on unit productivity. Using numerical approaches such as CFD to model the multiphase reacting flow conditions offers the opportunity explore design and process decisions without risk and at drastically-lower costs.

Golchert et al. [7] created a CFD analysis of a secondary aluminum reverberatory furnace. The model focuses on the combustion gas space to simulate the fuel combustion, heat transfer, and pollutants/gas flow. Exploration of burner configuration using this model shows improvement to heat transfer when the burners were angled slightly downwards to counter the natural lift of the flame. Also focusing on the combustion gas space, Anderson et al. [8] performed simulations of a secondary lead reverberatory furnace to examine the potential impacts of the burden shape on potential productivity and refractory wear due to flame impingement, thus providing insight into charging behavior and burner positioning.

Numerical exploration of melting and smelting presents inherent difficulties for pyrometallurgical furnaces. Simplifications are often made to ensure numerical stability or to reduce complexity for the sake of computational resources or compute time. Buchholz and Rodseth [9] implemented an artificial heat sink on the aluminum product within the simulation of an aluminum reverberatory furnace. This allowed

for the approximation of the absorption of the heat of fusion that occurs in the actual process while allowing for both a steady-state process and a static domain (i.e. no material phase change from the melting product).

This work takes a similar approach to model a secondary lead reverberatory furnace. However, the methodology has been adapted for additional considerations needed to approximate the heat transfer of several melting/smelting reactions. Extending off the previous work of this author [10], mechanisms are implemented for the release of off-gases that occur during furnace operation. With these behaviors, a model of the furnace is created that allows for exploration of design decisions and their impact on productivity while still modeling only the combustion gas space.

## Methodology

The simulation model is created in ANSYS Fluent 2022R1 as a 3D, multiphase, steady-state simulation. Turbulence behavior is captured using the SST k-omega RANS turbulence model. The burners are directly modeled, with combustion occurring via the finite-rate/eddy-dissipation concept. Radiative heat transfer is considered using the P1 radiation model. In addition to its use in combustion, the species transport model is used for the off-gassing portion of the pseudo-reaction modeling. As mentioned above, no melting model is considered in this study and only the combustion gas space is included. Combustion of the natural gas fuel was modeled as a two-step reaction, with burner inputs taken from furnace operational conditions corresponding to the temperature and flue gas data used for model tuning.

Currently, not all the information needed to directly model the melting/smelting reactions of the charged material is known. Thus, the primary focus of this work is on the application of a "pseudo-reaction" condition that approximates a few macro-scale behaviors that occur during these reactions. Specifically, the model seeks to replicate the significant temperature changes and off-gas generation that occur.

### *Domain*

With the simulation isolated to the combustion gas space alone, the numerical model consists of mass flow inlets within the burners and a single pressure outlet at the flue duct. The lead and slag tap holes are excluded from this study. A diagram of the furnace domain in this study is shown in Fig. 1. The furnace front contains the burners, the pile of charged burden material, and a small amount of slag/bath surface. The rear of the furnace has the slag/bath surface and the flue. All sides excluding the openings and bottom surfaces are composed of refractory bricks. These bricks are modeled as flat surfaces with thicknesses and convective heat losses defined within the simulation.

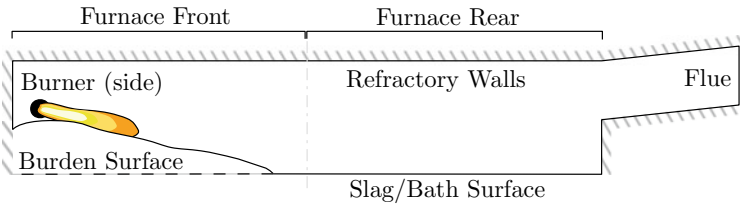


**Fig. 1** Side view of furnace CFD domain

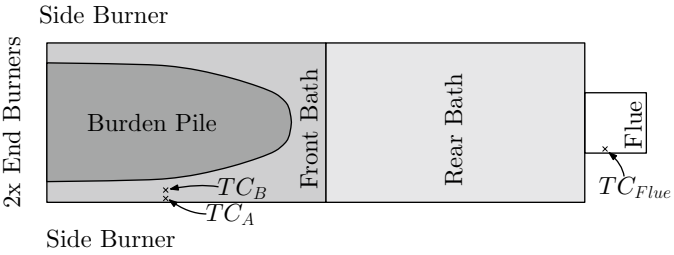


**Fig. 2** Top-down view of domain lower surfaces and thermocouple locations

The bottom surface comprises three areas: the burden, the front bath, and the rear bath. The transition from front bath to rear bath occurs at roughly halfway down the length of the furnace. The diagram in Fig. 2 shows the extent of these regions. The burden pile is the portion of charged material that is not submerged within the bath, the shape of which is replicated from measurements of side slope angles, heights of the "spine" along the central axis, and distance from the side walls at several points. Also seen in the diagram are the locations of the three thermocouples used for tuning the behavior the model.

The numerical grid consists of roughly six million polyhedral cells. The cell zone for the combustion space within the furnace is divided into four zones: the overall area combustion gas space of the furnace and a zone for each of the three lower surfaces made by isolating the first three cells neighboring those respective surfaces. These isolated cell zones are used for applying the pseudo-reaction source terms within the simulation, allowing each zone to be treated separately (a necessary consideration due to differences in their behavior).

## *Heat Transfer Subroutine*

The pseudo-reaction methodology consists of using user-defined subroutines to modify the behavior of a base simulation such that the impacts of smelting and melting reactions are included without the direct modeling of said reactions. For the study of the reverberatory furnace, the two primary factors missed by not modeling the

**Table 1** Charge material reactions and pseudo-reaction coefficients

| $i$ | Reaction | $A_i$ (kJK) | $B_i$ (kJ) | $T_{\text{ref}}$ (K) |
|---|---|---|---|---|
| 1 | $PbCO_3 \rightarrow PbO(s) + CO_2$ (g) | −0.084 | 39.01 | 588 |
| 2 | $PbSO_4 + 2C \rightarrow PbS + 2CO_2$ (g) | −0.111 | 21.25 | 923 |
| 3 | $Pb(OH)_2 \rightarrow PbO + H_2O$ (g) | 0.035 | 55.51 | 373 |
| 4 | $2\,PbO + PbS \rightarrow 3\,Pb + SO_2$ (g) | −0.294 | 237.7 | 1073 |
| 5 | $2\,PbO + C \rightarrow 2\,Pb + CO_2$ (g) | −0.156 | 43.94 | 873 |

reactions directly are the exo- and endo-thermic temperature changes caused by the reactions and the off-gases produced by said reactions. The approximation of energy changes within the model was explored by the authors in their previous work [10], wherein surface conditions on the burden and bath were adjusted such that temperatures within the simulation matched measurements taken from furnace operations.

In short, the approach uses artificial heat sinks defined within the simulation using user-defined functions (UDFs) as energy source terms. Each zone has separately-defined heat sinks based on the expected physical behavior of the zone. For the burden, the enthalpy changes and reaction temperatures for each of the five reactions (seen in Table 1) are used to determine the strength of these heat sinks. These are used to generate an approximate linear rate of enthalpy changes across a range of temperatures. Within the UDF, the cell's temperature is compared against each reaction temperature, adding to the sum total of enthalpy change expected within that cell for each matching condition. The equation of this is shown in Eqs. 1, where $\alpha_{\text{sink}}$ is a constant that is used to globally tune this behavior.

The rear bath does not have any reactions, thus its condition is a much-simpler linear behavior based on the difference between the cell temperature and the lead liquidus temperature (and also with a scaling factor $k_{\text{sink}}$ for adjustment) as seen in Eq. 2. The front bath uses a blend of these two conditions to reflect the submerged pile to the sides and front, with the front or rear behavior "fading" in based on cell position, as seen in Eqs. 3 and 4.

$$q_{\alpha_{\text{sink}}}(T) = -\alpha_{\text{sink}} \cdot \sum_{i=1}^{5} A_i (T - T_{\text{ref}_i}) + B_i \tag{1}$$

$$q_k(T_{\text{adj}}) = -k_{\text{sink}} \cdot (T - T_{\text{liq}}) \tag{2}$$

$$q_{\alpha_{\text{sink,front}}} = q_{\alpha_{\text{sink}}}(T) \cdot \max\left[\left(-\left(\frac{\bar{x} - \bar{x}_{\max}}{\bar{x}_{\max}}\right)^3 + 1\right), 0\right] \tag{3}$$

$$q_{k_{\text{sink,front}}} = q_{k_{\text{sink}}}(T) \cdot \max\left[\left(-\left(\frac{\bar{x}_{\max} - \bar{x}}{\bar{x}_{\max}}\right)^3 + 1\right), 0\right] \tag{4}$$

With the above behavior, the simulation of the reverberatory furnace can be given different burner inputs and result in different temperature profiles on the lower surface due to cells no longer meeting the requirements to "react". However, upon analyzing the resulting heat balance of the model, an issue was noticed. The relative amount of heat leaving the furnace via the flue gas was far lower than expected. Further analysis showed that the amount of mass leaving the flue was far less than what was measured. While the pseudo-reaction heat condition could alter temperatures, it was not generating the significant gaseous byproducts of the reactions.

## *Off-Gas Subroutine*

To overcome this limitation, a new feature was implemented into the pseudo-reaction code. Taking a similar approach as the heat-changing subroutine, off-gas generation subroutine would use the temperature data of marked cells (this time only above the burden pile) to determine if material needs to be generated. For each cell, the cell temperature is compared to the reaction temperatures of the reactions in Table 1. If the required condition is met, an amount of the resulting gas would be marked for generation. There were only three species to consider for this: $CO_2$ from reactions 1, 2, and 5, $H_2O$ from reaction 3, and $SO_2$ from reaction 4. The $SO_2$ species is unique in that it will only generate within the domain due to the burden reactions, as the other two are also byproducts of the burner combustion.

As with the temperature data tuning via comparison with thermocouples, flue gas measurements allowed for tuning of the off-gas condition. However, while the temperature condition required only two tuning coefficients ($\alpha$ and $k$), the species condition required four: $\beta_c$ for $CO_2$, $\beta_h$ for $H_2O$, $\beta_s$ for $SO_2$, and $\gamma$ for the amount of mass generated. The $\beta$ values are used to adjust the amount of species "generated" within the marked cells, as without the consideration of material consumption or reaction rates there is no way to quantify the relative differences in reactant quantity. With these $\beta$ terms, each of the three separate off-gas species can be individually adjusted as needed.

In ANSYS Fluent, defining a source term for a species forces a species fraction but does not generate mass to match. Therefore, after determining how much of each species is generated within a particular cell, a *DEFINE_ADJUST* subroutine is executed to calculate a total amount of mass to be generated within the cell. This value is multiplied by the $\gamma$ constant to scale the mass generation up or down as needed to match the known flue gas flow rate. A diagram of the UDF logic is shown in Fig. 3.

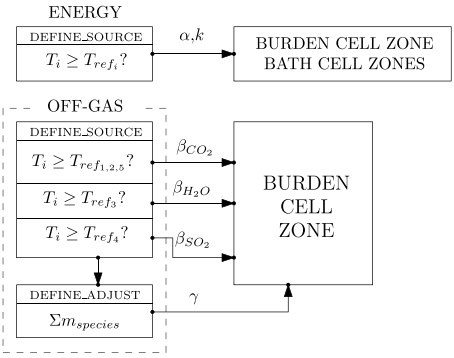


**Fig. 3** UDF procedure for energy and off-gas behaviors

## Results

As mentioned earlier, the pseudo-reaction behavior is tuned relative to data gathered from operation of the reverberatory furnace. The energy-adjustment subroutine is tuned such that temperature measurements within the simulation match measured values from three thermocouples (two near the burden pile and one within the flue). The previous efforts using only the energy-adjusting behavior [10] required tuning of the $\alpha$ and $k$ terms to match the thermocouples. The relationship between the temperatures within the model and those parameters (mostly $\alpha$) was nearly linear.

However, upon adding the off-gas generation behavior, differences were noted in both the temperature profiles of the system and the simulation's response to the tuning coefficients. The two systems (energy and off-gas) are inherently linked; a change in temperature results in an altered distribution/concentration of off-gasses which in turn affect the thermal properties of the combustion gas thus affecting the movement of heat within the domain. This leads to a more-difficult balancing act between the coefficients and the target values.

Figure 4 shows contours of temperature (normalized relative to global minimum and maximum values) on the lower surfaces of the furnace. Colder regions can be seen in the back of the burden pile and in the front of the pile that is only indirectly exposed to the heat from the burners. The spine of the burden pile is also at a slightly-lower temperature. The highest temperatures can be seen on the sides of the pile directly where the flames of the side burners impinge upon the burden material.

Plotting the strength of the pseudo-reaction's energy removal, an interesting pattern appears. Due to the nature of the enthalpy-based coefficients for each reaction, the regions with the highest temperatures do not correspond to the areas with the strongest degree of heat removal. As seen in Fig. 5, two "rings" of high energy removal exist near the peripheries of the burner impingement zones. With the exception of the third reaction (which remains endothermic), the reactions transition from endothermic behavior to exothermic behavior at various temperatures. At a temperature of approximately 1600 K a transition point is reached where the endothermic

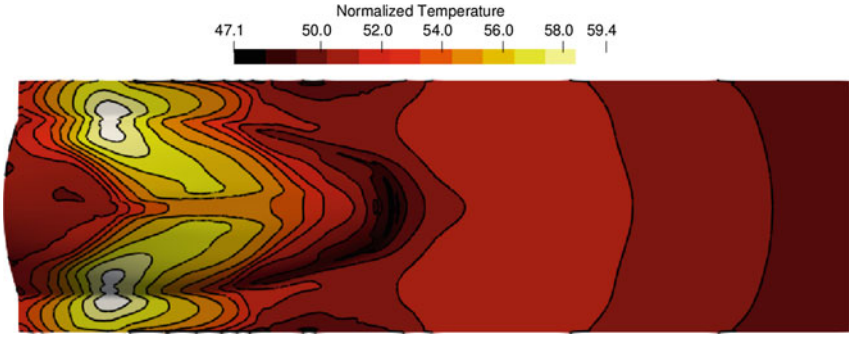


**Fig. 4** Locally-scaled contours of normalized temperatures on lower surfaces

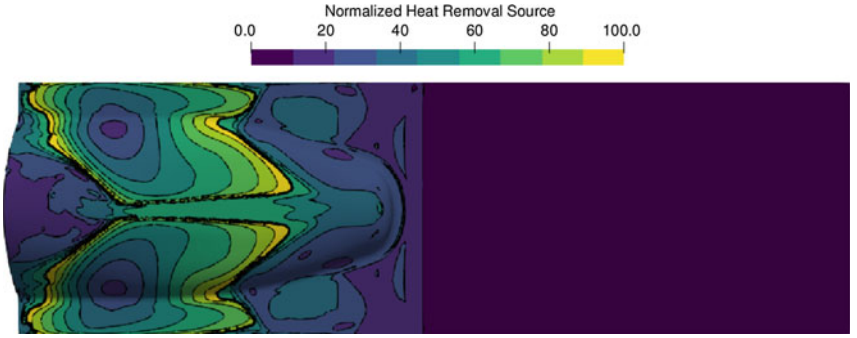


**Fig. 5** Contours of pseudo-reaction energy source term on lower surfaces

and exothermic behaviors of all five reactions cancel each other out. This leads to a natural balancing effect in some regions of the burden pile.

As the $SO_2$ in the system is only sourced from the pseudo-reaction source term, contours of $SO_2$ concentration along the center plane of the domain provide some insight into the behavior approximated reactions. Figure 6 shows the off-gassing of the $SO_2$ from the burden surface, with the gas flow of the furnace driving the emissions towards the flue. The rear of the burden pile produces very little $SO_2$, likely due to the lower temperatures as the reaction which produces the $SO_2$ has the highest reaction temperature of the five reactions in the model.

The resulting composition of the flue gas after tuning the coefficients was within desired ranges for both the concentration of the target species as well as for the overall mass flow rate. Table 2 shows the resulting error in the model results relative to the measured data from furnace operations. The highest error seen is for the oxygen content of the flue versus the simulation. One aspect of the reactions that is not currently considered is the consumption of oxygen by the coke in Reaction 5. In operational measurements, flue gas volume of oxygen was found to be between

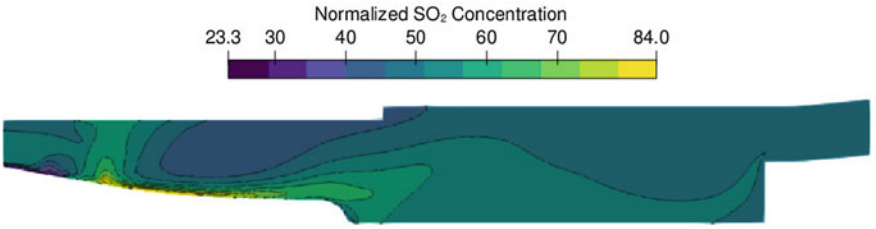


**Fig. 6** Side view center plane contours of normalized $SO_2$ concentration

**Table 2** Flue gas composition and flow rate error relative to operations

| | $H_2O$ | $CO_2$ | $O_2$ | $SO_2$ | $\dot{m}_{\text{flue}}$ |
|---|---|---|---|---|---|
| **Error %** | 9% | 7% | 69%+ | 3% | 5% |

**Table 3** Heat balance error relative to operations

| Case | Reactions (%) | Walls (%) | Cooling (%) | Flue (%) | Total (%) |
|---|---|---|---|---|---|
| No Off-Gas | +65 | −70 | −57 | −45 | +7 |
| Off-Gas | <1 | −33 | −54 | −9 | +7 |

**Table 4** Thermocouple temperature error relative to operations

| Case | $TC_A$ (%) | $TC_B$ (%) | $TC_F$ (%) |
|---|---|---|---|
| No off-gas | 1 | 2 | 1 |
| Off-gas | 0 | 2 | 11 |

0–4% (averaged to 2% for this analysis) while the simulation shows roughly 5% of flue output being oxygen.

Looking at the resulting heat removal within the furnace, Table 3 shows the impact of the off-gas inclusion in the pseudo-reaction model. It is estimated that 30–40% of the heat from the combustion sources is consumed by the melting and smelting processes. Comparing the previous pseudo-reaction simulation (without off-gassing) to a heat balance of the operating furnace, reactions and super-heating of the bath went from an over-prediction of roughly 65% (62% of combustion input) to nearly matching the estimation. The accuracy of heat removal via the walls also improved, though the error in heat removed via cooling elements remained unchanged. The heat removal via flue gasses is still slightly under-predicted but is much improved over the simulation without off-gas consideration.

One noticeable impact of the off-gas inclusion was an increased sensitivity to the adjustment of the $\alpha_{\text{sink}}$ value for the burden and bath energy removal. Previously, the $\alpha_{\text{sink}}$ term was found to have an almost-linear impact on the temperatures at the front and rear of the furnace. However, the addition of the off-gas species resulted

in much greater changes at the front area of the furnace (at the two burden-adjacent thermocouples) versus the rear (flue thermocouple) region, with flue temperatures remaining close to the target value but front values plummeting at higher values of $\alpha_{\text{sink}}$.

While the energy loss-only study used an $\alpha_{\text{sink}}$ of 70 to obtain a temperature match to the thermocouple data, the off-gas study required a lowering of the value to 40. Even then, Table 4 shows errors in temperature measurements increased from between 1–2% error up to as much as 11% error, with flue temperatures being much higher. This behavior is currently being investigated by the authors, but may be due to the "doubling-up" of heat removal via the source term and generation of new mass in the cell, wherein added mass alters the impact of the energy source term as applied by ANSYS Fluent as well as the increased heat capacity of the species-laden gas convecting more heat away from the burden region.

Interestingly, the error for overall heat losses within the furnace remained the same between the two simulations, indicating that the heat previously removed by the energy subroutine is now being transported by the generated species to exit at the flue.

## Conclusions

In this work, a numerical subroutine was developed and applied to the steady-state simulation of a secondary lead reverberatory furnace. Aiming to replicate the macro-behaviors of the melting and smelting reactions from the conversion of the charge materials into liquid lead, a pseudo-reaction was used to alter the heat balance within the furnace as well as generate off-gasses that would occur during the process. The current model has been adjusted to match the measured behaviors of the operational furnace, with further work underway to validate and explore the model. Once validated, the simplifications made within this model will allow for faster modeling of furnace conditions, including exploration of furnace design and burner set points.

**Acknowledgements** This work was funded by Research Award No. W911NF1920108 from the Army Research Laboratories of the Department of Defense and the Worcester Polytechnic Institute. The authors would also like to extend their gratitude for Gopher Resource in providing information on design, operational conditions, measurement data, and process insight.

## References

1. U.S. Geological Survey: Mineral commodity summaries 2021. Technical report, U.S. Geological Survey, Reston, VA (2021). https://doi.org/10.3133/mcs2021. https://pubs.er.usgs.gov/publication/mcs2021
2. Gottesfeld P, Pokhrel AK (2011) Review: lead exposure in battery manufacturing and recycling in developing countries and among children in nearby communities. J Occupat Environ Hyg 8(9):520–532

3. Queneau PB, Leiby R, Robinson R (2015) Recycling lead and zinc in the United States. World Metall ERZMETALL 68(3):149–162
4. Davidson AJ, Binks SP, Gediga J (2016) Lead industry life cycle studies: environmental impact and life cycle assessment of lead battery and architectural sheet production. Int J Life Cycle Assess 21(11):1624–1636
5. King PE, Hayes MC, Li T, Han Q, Hassan M, Golchert BM (2005) Design and operation of an experimental reverberatory aluminum furnace (2005)
6. Kumar A, Venuturumilli R, Kiss L, Walter G (2008) Experimental and numerical study of flame load heat transfer in an experimental furnace
7. Golchert BM, Zhou CQ, Quenette A, Han Q, King PE (2005) Combustion space modeling of an aluminum furnace, pp 887–892
8. Anderson A, Grogan J, Bogin G, Taylor P (2018) Computational Modeling of a secondary lead reverberatory furnace: effect of burden geometry. In: Davis BR, Moats MS, Wang S (eds) Extraction 2018. Springer, Ottawa, Ontario, Canada, pp 881–890. https://doi.org/10.1007/978-3-319-95022-8_70
9. Buchholz A, Rodseth J (2011) Investigation of heat transfer conditions in a reverberatory melting furnace by numerical modeling. Light Metals 2011:1179–1184
10. Walla NJ, Anisiuba V, Silaen AK, Anderson A, Grogan J, Zhou CQ (2022) Boundary conditions for modeling of a lead reverberatory furnace. In: ASME 2022 heat transfer summer conference, p. 8. American Society of Mechanical Engineers, Philadelphia, Pennsylvania, USA (2022). https://doi.org/10.1115/HT2022-81206. https://asmedigitalcollection.asme.org/HT/proceedings/HT2022/85796/V001T18A002/1146590

# Effect of Wearing Impellers on Multiphase Flow and Desulfurization During KR Mechanical Stirring Process


**Wei Chen, Yanyu Zhao, and Lifeng Zhang**

**Abstract** It is of great significance to study the variation of the multiphase flow during the entire service process of an impeller to improve the dispersion of the desulfurizer and the desulfurization efficiency during the KR desulfurization process. In the current study, the key dimensions of an actual KR impeller during the service process were quantitatively measured first. Then, a three-dimensional model coupled with the $k$-$\varepsilon$ turbulence model, VOF multiphase flow model, DPM model, UDS model, and unreacted core desulfurization model was established to predict the multiphase flow and desulfurization during the KR mechanical stirring process with different wearing impellers. The results show that with the increase of the wear degree of the impeller, the stirring effect was gradually weakened, resulting in a gradual weakening of the desulfurization efficiency. The desulfurization end sulfur content was 58.2 ppm after the impeller employed 220 heats, which was more than 4 times higher than the 13.0 ppm with a new impeller.

**Keywords** Wearing impellers · Multiphase flow · Desulfurization · KR process

## Introduction

The KR mechanical stirring method has obvious advantages in the desulfurization effect and desulfurization cycle due to its superior kinetic conditions and is widely used in the hot metal pretreatment desulfurization process [1, 2]. Many researches about the fluid flow and desulfurization during the KR process have been published. Ji [3] used the Euler-granular model to study the mixing of the desulfurizer and

W. Chen
School of Mechanical Engineering, Yanshan University, Qinhuangdao 066004, China

Y. Zhao
Beijing Shougang Co., Ltd, Qianan, Hebei 064404, China

L. Zhang (✉)
School of Mechanical and Materials Engineering, North China University of Technology, Beijing 100144, China
e-mail: zhanglifeng@ncut.edu.cn



S. Wagstaff et al. (eds.), *Materials Processing Fundamentals 2023*, The Minerals, Metals & Materials Series, https://doi.org/10.1007/978-3-031-22657-1_2

high-sulfur hot metal under the variable-velocity stirring method. The effect of the impeller geometry on the fluid flow and particle volume fraction was investigated [4]. Li [5] developed a coupled $k$-$\varepsilon$ model and VOF model to get insight into the flow pattern and interface behavior taking place during the KR desulfurization process. It shows that the interface profile and vortex depth strongly depend on the impeller dimension. Wang [6] established a transient-coupled three-dimensional numerical model to study the two-phase flow, heat transfer, desulfurizer motion, and desulfurization behavior during the KR hot metal treatment. He [7] studied the distribution and motion behavior of desulfurizers in a 170 t hot metal ladle with KR mechanical stirring using the Eulerian–Lagrangian approach. Nakaoka [8] investigated the fluid flow and particle transport accompanied by turbulent agglomeration using numerical simulation. It can be seen that most of the research was concerned with the fluid flow, vortex distribution, and particle dispersion. In addition, most of the published studies on the hot metal desulfurization were theoretical analyses and experimental observations applicable to special conditions [9, 10]. However, the desulfurization model with a wider scope needed to further couple the numerical simulation of the fluid flow and the desulfurization kinetic model, but this part of the research was still relatively few. The effect of the wear degree of the impeller on the flow field and desulfurization also needed further study [11].

In the current study, a three-dimensional model coupled with the $k$-$\varepsilon$ turbulence model, VOF multiphase flow model, DPM model, UDS model, and unreacted core desulfurization model was established to investigate the effect of the impeller wear degree on the multiphase flow and desulfurization in a 250 t KR hot metal ladle.

## Mathematical Model

A three-dimensional model based on a 250 t KR hot metal ladle was established, as shown in Fig. 1. The range of rotation speed and immersion depth of the impeller in the actual production process was 90–110 rpm and 1500–1700 mm, respectively. The upper and lower diameter of the hot metal ladle after removing the refractory part was 4066 mm and 3738 mm. The total number of grids of the current mold was about 0.5 million. Other specific model parameters and boundary conditions can be found in the previous study [12].

The upper and lower rotation diameter of the initial unused impeller in Fig. 1 were 1400 mm and 1300 mm, respectively. The height and width were 950 and 480 mm. As the stirring time increased, the employed impeller was gradually eroded by the hot metal and slag. In addition, the desulfurization slag also adhered to the impeller. Figure 2 shows the morphology of the same impeller with the initial state (left), after employed 120 heats (middle), and after employed 220 heats (right). The service life of the impeller was about 270 heats, and the results in Fig. 2 show that the impeller was severely eroded after employed 220 heats. Therefore, the above impellers were modeled and their effects on the flow field and desulfurization were investigated.